Comparison of Aeroelastic Modeling and Robust Flutter Analysis of a Typical Section ⋆

A. Iannelli * **A. Marcos** * **M. Lowenberg** *

* *University of Bristol, BS8 1TR, United Kingdom*
(e-mail: andrea.iannelli/andres.marcos/m.lowenberg@bristol.ac.uk).

Abstract: A comparison of robust flutter analyses within the μ framework is presented. The chosen test bed is the typical section with unsteady aerodynamic loads, which enables basic modeling features to be captured and so extend the gained knowledge to practical problems treated with modern techniques. The two main approaches to pose the LFT problem are investigated and features such as numerical accuracy and physical uncertainty description are assessed. A criterion is proposed to correlate the families of plants originated by the uncertainty description of the aerodynamic operator when different approximation algorithms are employed.

Keywords: Robust stability, Flexible structures, Flutter analysis, Structured Singular Value

1. INTRODUCTION

The interaction among inertial and elastic forces in a mechanical system is the subject of structural dynamics. For systems such as lifting surfaces, blades or sails, the external loading is represented by aerodynamic forces. The study of these systems is then addressed by aeroelasticity, which investigates the coupled problem of a deformable structure surrounded by a fluid flow generating a pressure dependent on its geometry.

Flutter is a self-excited instability in which aerodynamic forces on a flexible body couple with its natural vibration modes producing oscillatory motion. The level of vibration may result in sufficiently large amplitudes to provoke failure and often this phenomenon dictates the design of the aerodynamic body. Thus, flutter analysis has been widely investigated and there are several techniques representing the state-of-practice (Edwards and Wieseman (2008)). The major methods, for example k and p-k method, are based on the frequency-domain as this is the framework in which the aerodynamic loads are more often expressed.

Despite the large amount of effort spent in understanding flutter, it is acknowledged that predictions based only on computational analyses are not totally reliable. Currently this is compensated by the addition of conservative safety margins to the analysis results and expensive flutter test campaigns. One of the main criticalities arises from the sensitivity of aeroelastic instability to small variations in parameter and modeling assumptions. In addressing this issue, in the last ten years researchers looked at robust modeling and analysis techniques from the robust control community, specifically linear fractional transformation (LFT) models and μ analysis (Packard and Doyle (1993); Balas et al. (1998)). The so-called flutter robust analysis aims to quantify the gap between the prediction of the nominal stability analysis (model without uncertainties) and the worst-case scenario when the whole set of uncertainty is contemplated. This is believed to be a powerful tool when used as a complement to the classical techniques in that it could highlight weak points of the model requiring more refinement and conversely identify parameters that can be coarsely estimated as they do not have a strong influence on the results. The most well-known robust flutter approaches are those from Lind and Brenner (2012), Borglund (2004), Idan et al. (1999), with the first even including on-line analysis during flight tests.

Each of the aforementioned robust flutter approaches used the same underlying μ analysis tools but a different LFT model development path, in addition to relying on different aerodynamic approximations (e.g. Roger or Minimum State). The goal of each of those robust flutter studies was to provide an end-to-end process, from robust modeling to robust analysis, and demonstrate the validity of the approach. Since this was their focus, no detailed study or comparison was performed on the effect the modeling choices have on the analysis –although it is well-known in the robust control community that this is a fundamental issue (Marcos and Balas (2004); Magni (2004); Marcos et al. (2015)). Thus, the goal of this article is to present a comparison of the modeling options and a better understanding of their effects on the flutter analysis.

The layout of the article is as follows. Section 2 presents the test bed adopted. This section also includes a cursory description of the algorithms employed for the aerodynamics rational approximations. Nominal flutter results are presented in Section 3 followed by a very brief description of LFT and μ analysis in Section 4. The comparison and discussion of results obtained with the different approaches is presented in Section 5, ending with the conclusions in Section 6.

⋆ This work has received funding from the European Union's Horizon 2020 research and innovation programme under grant agreement No 636307, project FLEXOP.

2. AEROELASTIC MODELING

2.1 Typical section

The *typical section* model was introduced in the early stages of aeroelasticity to investigate dynamic phenomena such as flutter (Bisplinghoff and Ashley (1962)). Despite its simplicity, it captures essential effects in a simple model representation, see Fig. 1.

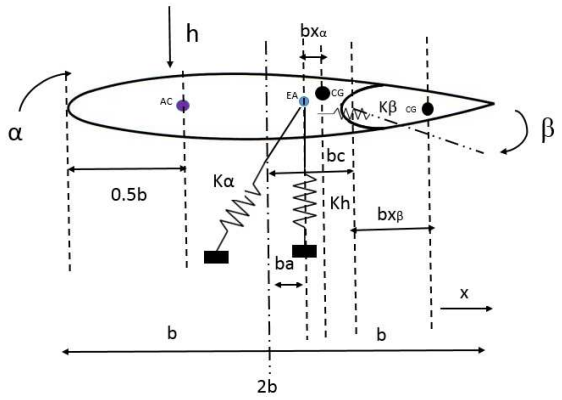

Fig. 1. Typical section sketch

From the structural side, it basically consists of a rigid airfoil with lumped springs simulating the 3 degrees of freedom of the section: plunge h, pitch α and trailing edge flap β. The positions of the elastic axis (EA), center of gravity (CG) and the aerodynamic center (AC) are also marked. The main parameters in the model, see Fig.1, are: K_h, K_α and K_β -respectively the bending, torsional and control surface stiffness; half chord b and dimensionless distances a, c from the mid-chord to respectively the flexural axis and the hinge location; x_α and x_β dimensionless distances from flexural axis and airfoil center of gravity and from hinge location and control surface center of gravity.

For the aerodynamic loads model, the unsteady formulation proposed by Theodorsen (1935) is employed. This approach is based on the assumption of a thin airfoil moving with small harmonic oscillations in a potential and incompressible flow. Despite its simplicity, such an aerodynamic force description is pertinent to flutter analysis since this is a condition of neutral stability of the system. The same hypotheses underline most of the other aerodynamic approaches (Doublet Lattice Method is an example) later developed to improve flutter analysis accuracy.

In order to present the basic model development approach, $\mathbf{X}$ and $\mathbf{L_a}$ are defined as the vectors of the degrees of freedom and of the aerodynamic loads respectively. The set of differential equations describing the dynamic equilibrium (Hodges and Pierce (2011)) can then be recast in matrix form using Lagrange's equations:

$$\big[\mathbf{M_s}\big]\ddot{\mathbf{X}} + \big[\mathbf{C_s}\big]\dot{\mathbf{X}} + \big[\mathbf{K_s}\big]\mathbf{X} = \mathbf{L_a} \tag{1}$$

where $\big[\mathbf{M_s}\big]$, $\big[\mathbf{C_s}\big]$ and $\big[\mathbf{K_s}\big]$ are respectively the structural mass, damping and stiffness matrices. The expression of $\mathbf{L_a}$, provided in the Laplace s domain, is:

$$\mathbf{L_a}(s) = q\big[\mathbf{A}(\bar{s})\big]\mathbf{X}(s) \tag{2}$$

where the dynamic pressure q and the dimensionless Laplace variable $\bar{s}$ ($=s\frac{b}{V}$ with V the wind speed) are introduced. $\big[\mathbf{A}(\bar{s})\big]$ is called the generalized Aerodynamic Influence Coefficient (AIC) matrix, and is composed of generic terms $\mathbf{A}(\bar{s})_{ij}$ representing the transfer function from each degree of freedom j in $\mathbf{X}(s)$ to each aerodynamic load component i in $\mathbf{L_a}(s)$.
It is remarked that Theodorsen's aerodynamic theory assumes harmonic motion, which means that the relation in (2) is pertinent only if $\big[\mathbf{A}(\bar{s})\big]$ is evaluated at $\bar{s}{=}i\omega\frac{b}{V}{=}ik$, where k is called the *reduced frequency*. The final aeroelastic equilibrium is given by:

$$\Big[\big[\mathbf{M_s}\big]s^2 + \big[\mathbf{C_s}\big]s + \big[\mathbf{K_s}\big]\Big]\mathbf{X} = q\big[\mathbf{A}(\bar{s})\big]\mathbf{X} \tag{3}$$

2.2 Rational Approximations

The AIC matrix does not have a rational dependence on the Laplace variable s and this forces approximations of the aerodynamic operator to be pursued in order to provide an expression for (3) in state space, which is essential to deal with aeroservoelastic problems. The difference between a quasi-steady and an unsteady formulation of the aerodynamic loads is that the latter attempts to model the memory effect of the flow, which results in phase shift and magnitude change of the loads with respect to the former one. This is commonly referred to as *time lag* effect. A general two-part approximation model can then be obtained based on *quasi-steady* (QS) and *lag* contributions:

$$\big[\mathbf{A}(\bar{s})\big] \approx \Gamma_{QS} + \Gamma_{lag} \tag{4}$$

In this paper two among the most established algorithms are presented: Roger method and Minimum State method. They propose a formally identical expression for Γ_{QS}:

$$\Gamma_{QS} = \big[\mathbf{A_2}\big]\bar{s}^2 + \big[\mathbf{A_1}\big]\bar{s} + \big[\mathbf{A_0}\big] \tag{5}$$

Where $\big[\mathbf{A_2}\big]$, $\big[\mathbf{A_1}\big]$ and $\big[\mathbf{A_0}\big]$ are real coefficient matrices.

Roger proposed (Roger (1977)) that Γ_{lag} could be approximated as:

$$\Gamma_{lag-Roger} = \sum_{L=3}^{N} \frac{\bar{s}}{\bar{s}+\gamma_{L-2}}\big[\mathbf{A_L}\big] \tag{6}$$

The partial fractions inside the summation are the so-called *lag terms* and they basically represent high-pass filters with the aerodynamic roots γ_i as cross-over frequencies. The real coefficient matrices $\big[\mathbf{A_i}\big]$ with $i = 0...N$ are found using a linear least-square technique for a term-by-term fitting of the aerodynamic operator. The resulting state-space equation includes augmented states representing the aerodynamic lags, which are equal to the number of roots multiplied by the number of degrees of freedom.

The MS method (Karpel (1981)) tries to improve the efficiency of Roger's in terms of number of augmented states per given accuracy of the approximation. There is no clear quantification of this advantage, but it has been stated (Idan et al. (1999)) that the number of aerodynamic states may typically be 6-8 times smaller for the same level of model accuracy. The Γ_{lag} expression is:

$$\Gamma_{lag-MS} = \big[\mathbf{D'}\big]\begin{bmatrix} \frac{1}{\bar{s}+\gamma_1} & \dots & 0 \\ \vdots & \ddots & \vdots \\ 0 & \dots & \frac{1}{\bar{s}+\gamma_{N-2}} \end{bmatrix}\big[\mathbf{E'}\big]\bar{s} \tag{7}$$

The coefficients of $\big[\mathbf{D'}\big]$ and $\big[\mathbf{E'}\big]$ are iteratively determined through a nonlinear least square since (7) is bilinear in

these two unknowns, while the matrices defining Γ_{QS} (5) are now obtained imposing the constraint to match the aerodynamic operator at k=0 and at another selected reduced frequency k_c. The number of augmented states is now equal to the number of roots.
The impact that the differences in the expression of Γ_{lag} have on robust flutter analysis when lag terms are uncertain will be investigated in Section 5.

Both methods lead to the same short-hand state matrix:

$$\begin{bmatrix} \dot{\hat{\mathbf{X}}}_\mathbf{s} \\ \dot{\hat{\mathbf{X}}}_\mathbf{a} \end{bmatrix} = \begin{bmatrix} \boldsymbol{\chi_{ss}} & \boldsymbol{\chi_{sa}} \\ \boldsymbol{\chi_{as}} & \boldsymbol{\chi_{aa}} \end{bmatrix} \begin{bmatrix} \hat{\mathbf{X}}_\mathbf{s} \\ \hat{\mathbf{X}}_\mathbf{a} \end{bmatrix} \tag{8}$$

Where $\hat{\mathbf{X}}_\mathbf{s}$ and $\hat{\mathbf{X}}_\mathbf{a}$ are respectively the vector of structural and aerodynamic states.

3. NOMINAL FLUTTER ANALYSIS

Nominal flutter analysis studies the conditions at which the dynamic aeroelastic system loses its stability. As the air stream speed V varies the system's behavior in terms of response and stability changes. The result is the prediction of the so-called flutter speed V_f, below which the system is guaranteed to be stable.

In principle it is possible to solve the problem studying either (3) or (8). In the later case, the stability of the system is related to the spectrum of the state-matrix. We will use the Roger and MS approximations for nominal comparison. In the former case (the most reliable and currently adopted approach), the objective is to find the flutter determinant roots s such that nonzero solutions for $\mathbf{X}$ exist. The complexity arises since $\left[\mathbf{A}(\bar{s})\right]$ does not have a polynomial dependence on s and thus iterative solutions have to be sought. We will use the p-k method to baseline the comparison.

The parameter values for these analyses are taken from (Karpel (1981)). In Fig. 2 the eigenvalues corresponding to the structural modes are depicted as speed increases. The system exhibits a plunge-torsion flutter, featured by the merging of the frequencies just before instability occurrence (*binary flutter*). Table 1 summarizes the results. For the Roger method, 4 aerodynamic roots equally spaced between -0.1 and -0.6 were selected (state-matrix size equals 18), while for the MS method 5 aerodynamic roots equally spaced in the same range were used (state-matrix size equals 11). No substantial mismatches are found in the flutter speeds.

	Flutter velocity $[\frac{m}{s}]$	Flutter frequency $[Hz]$
State Space - Roger	302.7	11.25
State Space - MS	302.5	11.2
Frequency-domain p-k	301.8	11.2
Ref. Karpel (1981)	303.3	11.15

Table 1. Nominal flutter analyses results

4. LFT AND μ ANALYSIS

In this section a very cursory presentation of the mathematical concepts behind linear fractional transformation (LFT) modeling and robust μ analysis is given. The interested reader is referred to Packard and Doyle (1993); Balas et al. (1998).

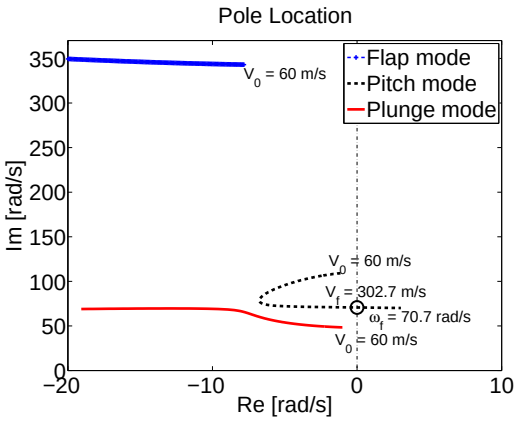

Fig. 2. Nominal system: pole locations in terms of speed

If the *coefficient matrix* $\mathbf{M}$ is defined as a proper transfer matrix, $\mathcal{F}_u$, namely the upper LFT, is the closed-loop transfer matrix from input $\mathbf{u}$ to output $\mathbf{y}$ when the nominal plant $\mathbf{M_{22}}$ is subject to a perturbation matrix $\boldsymbol{\Delta}$ (Fig. 3). $\mathbf{M_{11}}$,$\mathbf{M_{12}}$ and $\mathbf{M_{21}}$ reflect a priori knowledge of how the

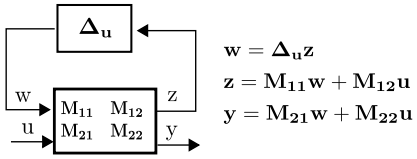

Fig. 3. Lower and upper LFTs

perturbation affects the nominal map. Once all varying or uncertain parameters are *pulled out* of the nominal plant, the problem appears as a nominal system subject to an artificial feedback. The algebraic expression for $\mathcal{F}_u$ is given by:

$$\mathcal{F}_u(\mathbf{M}, \boldsymbol{\Delta_u}) = \mathbf{M_{22}} + \mathbf{M_{21}}\boldsymbol{\Delta_u}(\mathbf{I} - \mathbf{M_{11}}\boldsymbol{\Delta_u})^{-1}\mathbf{M_{12}} \tag{9}$$

This LFT is well posed if and only if the inverse of $(\mathbf{I} - \mathbf{M_{11}}\boldsymbol{\Delta_u})$ exists.

The structured singular value (s.s.v.) is a matrix function denoted by $\mu_\Delta(M)$ and defined as:

$$\mu_\Delta(M) = \frac{1}{\min_\Delta(\bar{\sigma}(\Delta) : \det(I - M\Delta) = 0)} \tag{10}$$

where $\bar{\sigma}(\Delta)$ is the maximum singular value of Δ. Note that this definition can be specialized to determine whether the LFT $\mathcal{F}_u(\mathbf{M}, \boldsymbol{\Delta})$ is well posed once the generic matrix M in the above definition is replaced by $\mathbf{M_{11}}$ and Δ belongs to the corresponding uncertainty set $\boldsymbol{\Delta}$. For ease of calculation and interpretation, Δ is typically norm-bounded $\|\Delta\|_\infty < 1$ (without loss of generality by scaling of M). In this manner, if $\mu_\Delta(M) \leq 1$ then the result guarantees that the analyzed system represented by the LFT is robust to the considered uncertainty level. The structured singular value is a robust stability (RS) test but can be used also for robust performance (RP).

It is known that $\mu_\Delta(M)$ is non-polynomial (NP) hard with either pure real or mixed real-complex uncertainties, thus the algorithms implement upper and lower bound calculations (Balas et al. (1998)). The upper bound μ_{UB} provides the maximum size perturbation for which RS/RP is guaranteed, while the lower bound μ_{LB} guarantees the minimum size perturbation for which RS/RP is guaranteed to be violated. Along with this information, the lower

bound also provides the matrix $\Delta_{LB} = \Delta_{cr}$ satisfying the determinant condition.

5. ROBUST FLUTTER ANALYSIS

Robust flutter analysis deals with flutter instability predictions when the aeroelastic model is subject to uncertainties. Examples of the latter are low confidence in the values of parameters and coefficients of the matrices, or neglected dynamics in the nominal model. Once a quantification of the uncertainty and its mathematical description are provided by means of LFT, μ analysis enables to predict at a given speed if the set of uncertainties is capable of leading to instability.

5.1 General preamble on flutter analysis with μ

The standard μ framework applies to systems represented by rational transfer function matrices (or similarly described by ODE), which are easily recast in state-space. This is related to the existence of well established state-space algorithms employed in servo-control applications and marked the path for the development of the first robust flutter μ analyses. But in fact, the μ technique and the intimately related concept of LFT are frequency-domain based. Recalling (9), the core problem is to study the well-posedness of the LFT describing a representative transfer function of the plant. What can be different is the LFT model development path applied. That is, either (3) or (8) can be taken as a starting point to develop the proper LFT framework. In this work both approaches are investigated, trying to highlight benefits and shortcomings.

The considered uncertainties are of a *multiplicative* type. This means that the generic uncertain parameter C is written as $C = C^0(1 + \sigma_C \delta_C)$ where σ_C defines the uncertainty level, $\delta_C \in [-1, 1]$ and δ_C=0 corresponds to the nominal value C^0. The LFT $\mathcal{F}_u(\mathbf{M}, \mathbf{\Delta_S})$ describing the plant affected by uncertainties in the structural parameters is the same for both approaches and it is characterized by the uncertainty block:

$$\mathbf{\Delta_S}^{5,R} = \text{diag}(\delta_{M_{s11}}, \delta_{M_{s12}} I_2, \delta_{M_s 22}, \delta_{K_s 11}, \delta_{K_s 22}) \quad (11)$$

where the size of the uncertainties and their nature (real R or complex C) is recalled in the superscripts. A range of 10% from the nominal value is defined for $\mathbf{M_{s11}}$, $\mathbf{M_{s22}}$ and $\mathbf{K_{s22}}$, while for $\mathbf{M_{s12}}$ and $\mathbf{K_{s11}}$ it is 1%.
It is well known (Packard and Doyle (1993)) that calculation with pure real uncertainties of the upper bound is usually quite tight, while the accuracy of the lower bound highly depends on the nature of the $\mathbf{\Delta}$ matrix. It is desirable thus to formulate the problem in such a way that complex uncertainties can be introduced.
For uniformity, all the following analyses are performed at V=270$\frac{m}{s}$, which is 10% smaller than the nominal flutter speed. This choice is arbitrary since there is no interest in evaluating the safety margin degradation of a specific existent system.

5.2 State-space approach

This approach was firstly suggested by NASA (Lind and Brenner (2012)). The uncertainties are substituted in the state-matrix governing the nominal plant (8) so that the nominal dynamics is separated from the uncertain terms. In the present work this is accomplished by writing the uncertain parameters in symbolic form and using the well consolidated LFR toolbox (Magni (2004)) leading straightforwardly to an LFT representation of the uncertain system which is a valid input for μ analysis.

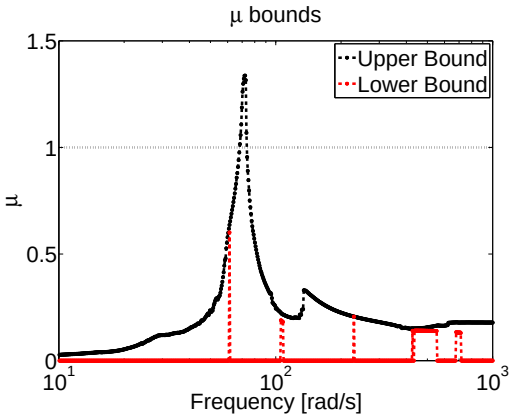

Fig. 4. Robust analysis: μ bounds for the case of structural $\mathbf{\Delta}$ in inertia and stiffness. State-space approach

In Fig. 4 the upper and lower bounds are reported for the case when only structural uncertainties are considered. The estimation given by μ_{UB} is that the system is flutter free for structural uncertainties up to approximately 75% ($\approx \frac{1}{1.35}$) of the assumed range, whereas no information is provided by μ_{LB} about the minimum size of the perturbation matrix which proves to cause plant instability.

Considering now errors in the aerodynamic model, generally uncertainties in the values of the lag roots are contemplated (Lind (2002)). Although these terms have the same physical meaning for Roger and MS methods, the way they enter the equations is different, as previously seen. An uncertainty of 5% in the value of the lag terms is considered in the analysis. Choice of number and nominal values for the roots reflects that of the nominal case. The uncertainty LFT block sizes are:

$$\begin{aligned} \mathbf{\Delta_{MS}}^{5,R} &= \text{diag}(\delta_{\gamma_1}, \delta_{\gamma_2}, \delta_{\gamma_3}, \delta_{\gamma_4}, \delta_{\gamma_5}) \\ \mathbf{\Delta_R}^{12,R} &= \text{diag}(\delta_{\gamma_1} I_3, \delta_{\gamma_2} I_3, \delta_{\gamma_3} I_3, \delta_{\gamma_4} I_3) \end{aligned} \quad (12)$$

Results are shown in Fig.5. Remarkably different margins of stability are predicted by the Roger and MS algorithms. In other words, the capability of the two families of aerodynamic operators to perturb the stability is considerably different when the same range of variation is allowed. Nonetheless robust predictions are expected to be identical as long as the aerodynamics' uncertainty descriptions are *consistent*. Consistency is here referred to a definition of the *range* of variation for the parameters such that the uncertainty operator $\mathbf{\Delta}$ maps the two approximations in two *similar* families of plants. A rationale to perform this range definition is here sought.

When the uncertainties are inserted in approximate operators, each of them can be represented as an upper LFT $\mathcal{F}(\hat{\mathbf{A}}, \mathbf{\Delta})$ (subscripts R and MS will be used to identify the two approximation options). It is known how the size of a transfer function (in terms of its H_∞ norm, i.e. the maximum singular value over the frequency range considered) affected by uncertainties can be determined using a μ robust stability test (Zhou et al. (1996)). This

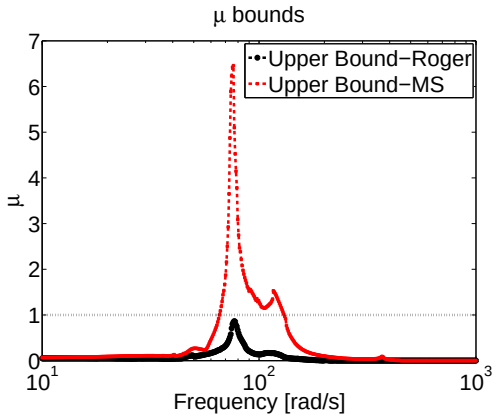

Fig. 5. Robust analysis: μ upper bounds for the case of aerodynamic $\mathbf{\Delta}$. State-space approach

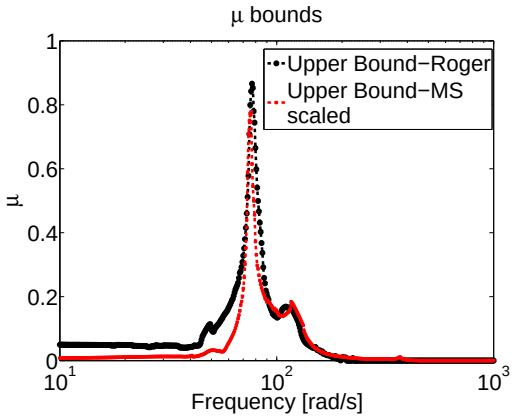

Fig. 6. Robust analysis: μ upper bounds for the case of aerodynamic $\mathbf{\Delta}$ with the range of variation of lag roots in MS approximation related to that of Roger according to the proposed criteria

procedure is generally employed in the calculation of robust performance. In particular the command *wcperf* of the μ toolbox (Balas et al. (1998)) estimates the norm $\bar{W}$ of the LFT $\mathcal{F}_u$ associated with a structured $\mathbf{\Delta}$ of size $\bar{\alpha}$:

$$\bar{W}(\mathcal{F}_u, \mathbf{\Delta}, \bar{\alpha}) = \|\mathcal{F}_u\|_\infty \tag{13}$$

Once defined a certain size $\bar{\alpha}$, $\bar{W}$ could represent a term of comparison among different uncertainty descriptions (and range definitions).

The proposed *validation* method is prompted by the observation of the two aerodynamic operators corresponding to the smallest perturbation leading to instability $\mathbf{\Delta}_{cr}$ in the studied cases. The corresponding values for Roger's $\|\mathbf{A}_R(\mathbf{\Delta}_{cr}^R)\|_\infty$ and Minimum State $\|\mathbf{A}_{MS}(\mathbf{\Delta}_{cr}^{MS})\|_\infty$ are respectively 13.3 and 13.7. These are just the values of $\|\mathcal{F}_R\|_\infty$ and $\|\mathcal{F}_{MS}\|_\infty$ when the corresponding sizes of uncertainty $\bar{\alpha}$ (respectively $\|\mathbf{\Delta}_{cr}^R\|_\infty$ and $\|\mathbf{\Delta}_{cr}^{MS}\|_\infty$) are defined.

Moreover, when the norm calculations are applied to the set adopted for the analyses reported in Fig. 5, fixing the size $\bar{\alpha}$=1, and considering a reduced frequency $k_T = 0.28$ (approximately the robust reduced flutter frequency), the values for $\|\mathcal{F}_R\|_\infty$ and $\|\mathcal{F}_{MS}\|_\infty$ are respectively 12.8 and 31. The discrepancies in the operator norms (despite identical nominal values) confirm that setting the *same* range of variation (5% in this case) for both of them lead to very different families of plant.

When the range of variation of the aerodynamic roots in $\mathcal{F}_{MS}$ is specified so as to lead to the same $\bar{W}$ (it is found that this range has to be about 9 times smaller than the one used in $\mathcal{F}_R$), the discrepancy in μ prediction falls within 10% (Fig. 6). This mismatch is thought to be caused by the discrepancies in H_∞ norm shown before (13.3 and 13.7 for the two different cases).

5.3 Frequency-domain approach

Recalling Section 4, the matrix used by μ analysis for well-posedness is $\mathbf{M_{11}}$. This is the transfer function seen by the perturbation block of the uncertain plant. Borglund (2004) proposed to perform the robust flutter analysis by starting from the plant formulated in the frequency-domain (3), with $\mathbf{M_{11}}$ *manually* assembled once the uncertain parameters are embedded. This procedure implies a gridding of the frequency range under investigation: for each discrete value ω in the range, the terms involved in the definition of $\mathbf{M_{11}}$ are constant matrices and then the algorithm for the calculation of μ can be initialized. Theoretically, the standard μ framework expressed through state-space doesn't need this discretization and thus it is capable of ensuring the absence of any discontinuities in the results. But the bounds algorithmic implementation implies this gridding. As a result, if the transfer functions involved in the uncertainty description have a rational dependence on the Laplace variable (as for the structural case), this procedure is identical to the former one. When the aerodynamics is affected by uncertainties, the two formulations are inherently different.

The main advantages of handling the analysis in this framework are discussed here. For a real aeronautical application (which relies on frequency-domain aerodynamic operators for flutter analyses) this approach ensures that both nominal and robust stability refers to the same starting equation (i.e. no approximations are inserted during the process). Uncertainties can be directly expressed in the *original* AIC matrix, and not in the operators defining the approximate expressions, enhancing physical considerations in the uncertain definition. Matrix coefficients are complex and so are the associated uncertainties, with notable improvement on the results accuracy. The weighting matrices defining the range of variation of the uncertainties can have whatever dependence on the frequency, while in the former approach the rational dependence constraint holds. An example of these features is provided in the following examples.

The case of only aerodynamic uncertainties is first examined. On the basis of the nominal flutter analysis which showed the merging of pitch and plunge modes at instability, the three more critical transfer functions are expected to be $\mathbf{A}_{12}$, $\mathbf{A}_{21}$ and $\mathbf{A}_{22}$. The uncertain description is such that *at each frequency* they range in the disc of the complex plane centered in the nominal value and having a radius equal to 10% of the absolute nominal value:

$$\mathbf{\Delta_A}^{3,C} = \mathrm{diag}(\delta_{A_{12}}, \delta_{A_{21}}, \delta_{A_{22}}) \tag{14}$$

The analysis for this plant is depicted in Fig.7. The most remarkable observation is that now lower and upper bounds coincide, leading to a precise estimation of the robust margin as opposed to that seen in Fig.4. The case of both structure and aerodynamic uncertainties,

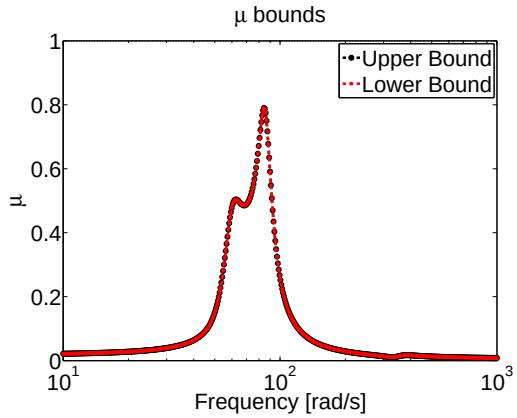

Fig. 7. Robust analysis: μ bounds for the case of only aerodynamic $\mathbf{\Delta}$. Frequency-domain approach

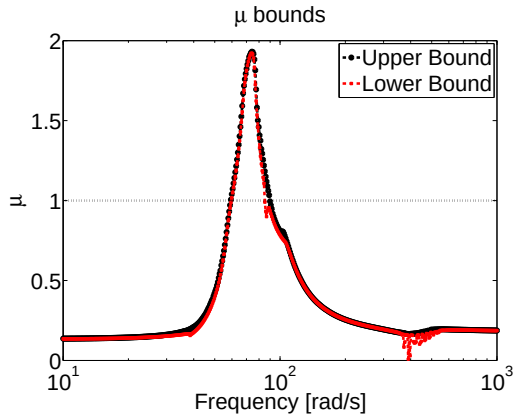

Fig. 8. Robust analysis: μ bounds for the case of mixed structural/aerodynamic $\mathbf{\Delta}$. Frequency-domain approach

obtained combining (11) and (14), is plotted in Fig. 8. This problem has mixed real and complex uncertainties, and the calculated μ bounds are tight. The information obtained through the perturbation matrix $\mathbf{\Delta_{cr}}$ can be useful to make design actions or sketch out control strategies for flutter suppression.

These results provide examples of the aforementioned advantages when modeling is entirely approached in the frequency-domain. It is worth remarking however that these comments are pertinent to robust flutter stability analysis. The scenario may change when other tasks are involved, for example robust control design for flutter suppression and/or on-line robust predictions during flight tests. Indeed, the latter has only been demonstrated using the state-space approach (Lind and Brenner (2012)) and well-consolidated algorithms could dictate the same way for the former task. These aspects deserve then a better insight, and could be addressed in the future.

6. CONCLUSION

This work attempts to compare techniques developed to study robust flutter analysis adopting the typical section with unsteady loads as a test bed. The investigations concern effect of the uncertainty description when two different aerodynamic approximations for the unsteady AIC matrix are employed. In the latter case, a criterion to select the range of variation for the parameters in order to define similar families of plants is proposed.

Numeric quality of lower and upper bounds calculation for different sets of uncertainties and framework where the problem is posed are highlighted. Advantages in terms of uncertainty description and results accuracy of the frequency-domain approach are assessed; the state-space approach on the other hand offers a more straightforward way to pose the problem, due to well established toolbox and a general greater confidence in the formulation of the plants in state-space. Although this is commonly true for control problems, the role played by the aerodynamics in the aeroelastic plant and its inherent frequency-domain expression could alter this scenario when these kind of stability analyses are pursued.

REFERENCES

Balas, G., Doyle, J., Glover, K., Packard, A., and Smith, R. (1998). *μ Analysis and Synthesis Toolbox*.

Bisplinghoff, R.L. and Ashley, H. (1962). *Principles of Aeroelasticity*. Wiley, New York.

Borglund, D. (2004). The μ-k method for robust flutter solutions. *Journal of Aircraft*, 41(5), 1209–1216.

Edwards, J.W. and Wieseman, C.D. (2008). Flutter and Divergence Analysis Using the Generalized Aeroelastic Analysis Method. *Journal of Aircraft*, 45(3), 906–915.

Hodges, D.H. and Pierce, G.A. (2011). *Introduction to Structural Dynamics and Aeroelasticity; 2nd ed.* Cambridge Aerospace series. Cambridge University Press, New York, NY.

Idan, M., Karpel, M., and Moulin, B. (1999). Aeroservoelastic Interaction Between Aircraft Structural and Control Design Schemes. *J. of Guidance, Control and Dynamics*, Vol. 22(No. 4), pp. 513–519.

Karpel, M. (1981). Design for Active and Passive Flutter Suppression and Gust alleviation. Technical Report 3482, NASA.

Lind, R. and Brenner, M. (2012). *Robust Aeroservoelastic Stability Analysis*. Advances in Industrial Control. Springer London.

Lind, R. (2002). Match-Point Solutions for Robust Flutter Analysis. 43rd AIAA/ASME/ASCE/AHS/ASC Structures, Structural Dynamics, and Materials Conference.

Magni, J. (2004). Linear Fractional Representation Toolbox Modelling, Order Reduction, Gain Scheduling. Technical Report TR 6/08162, DCSD, ONERA, Systems Control and Flight Dynamics Department.

Marcos, A. and Balas, G. (2004). Development of Linear Parameter Varying Models for Aircraft. *J. of Guidance, Control and Dynamics*, Vol. 27(No. 2), pp. 218–228.

Marcos, A., Bennani, S., Roux, C., and Valli, M. (2015). LPV modeling and LFT Uncertainty Identification for Robust Analysis: application to the VEGA Launcher during Atmospheric Phase. 1st IFAC Workshop on Linear Parameter Varying Systems, Grenoble, France.

Packard, A. and Doyle, J. (1993). The Complex Structured Singular Value. *Automatica*, 29(1), 71–109.

Roger, K. (1977). Airplane Math Modeling Methods for Active Control Design. *AGARD-CP-228*.

Theodorsen, T. (1935). General Theory of Aerodynamic Instability and the Mechanism of flutter. Technical Report 496, Naca.

Zhou, K., Doyle, J.C., and Glover, K. (1996). *Robust and Optimal Control*. Prentice-Hall, Inc., Upper Saddle River, NJ, USA.